Fault gouge porosity from 2D simulations of fractal particle size distribution

Reza Sehhati (1), Sujana Ganta (2), and Jafar Hadizadeh (3)
Civil and Environmental Engineering Department, University of Louisville
Reza.Sehhati@louisville.edu (1) Department of Computer Science and Computer Engineering, University of Louisville, (2) Department of Geography & Geosciences Department, University of Louisville (3)
This study is funded by NSF EAR-0229654 (Hadizadeh)

Summary

Two dimensional computer simulations were performed to determine porosity of various regions of experimental and natural gouges. The algorithm was without limitation on size and number of particles, and was designed to produce an equivalent texture with maximum packing density and a fractal particle size distribution. Porosity of the same gouge regions were also estimated by image processing method.

For initially angular gouge particle shapes the difference between measured and simulated porosity decreased significantly with increasing shear displacement. The porosity values determined by both methods sharply decreased over the initial increments of shear displacement and/or in transition from relatively undeformed regions into zones of shear localization. The fractal dimension increased with decreasing porosity.

The results suggest that particles in real gouge tend to become more equant in shape with increased shear and in regions of extreme comminution. The combination of particle shape changes and sharp decrease in local porosity results in increased packing densities and particle contacts. The expected increase in friction due to increased sliding surface area may not be sustainable because the loss of porosity associated with this process could result in a local cataclastic flow to fracture transition.

Objective

The shear localization process in fault gouge is not well understood. Intense comminution near and within zones of localized shearing results in increased contact surface area between gouge particles and should require higher shear stress for slip. The localization, however, is known to result in weakening of the gouge. We are testing the idea that shear localization might involve a localized cataclastic flow to fracture transition within highly comminuted regions where large porosity reductions occur.

Materials

Natural gouge

Gouge samples were collected from small-displacement faults in Aztec sandstone (Fig. 1a), Valley of Fire State Park (VOF), Nevada. The sandstone has an initial porosity of 24% to 29% and average particle size of 620 µm. The gouge thickness in the fault samples varied from 1 to 8.6 mm. Based on studies by Flodin & Aydin (2004) the prevailing pressure at the time of deformation was estimated to be ~10MPa. Further information about the VOF samples is given in Table 1.

Simulated gouge

Samples from three simulated Westerly granite gouge (Fig. 1b) experiments (WGK) were used in this study. The gouge was deformed at room temperature and 25 MPa normal stress to 44, 79, and 387mm of shear displacement in rotary shear apparatus. The initial porosity of the gouge was 35% with initial particle size of 88 µm. The gouge layers had a thickness of ~2 mm after initial compaction.

Fig.1

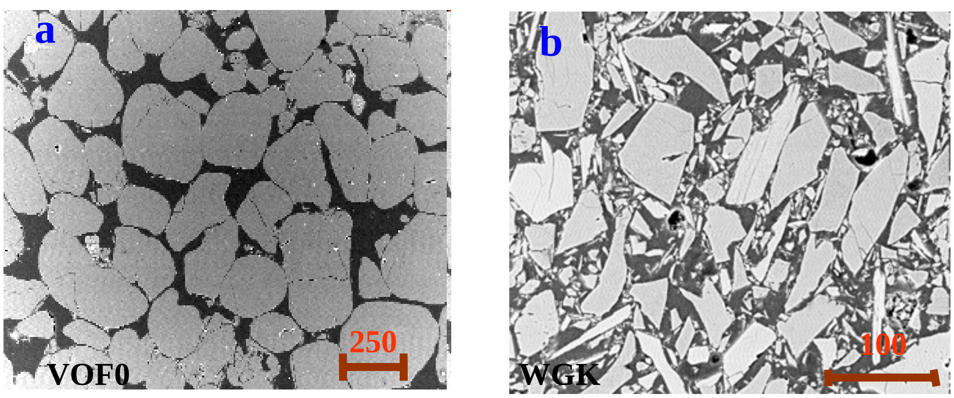

Table 1. Measurements of the small-displacement faults in Aztec sandstone

Sample	Shear Displacement (mm)	Thickness (mm)	γ_{avg}
3A	0	-	0
4a	17	1	17
2A	116	1.4	82.86
7	271	13	20.85
1	347	3.6	96.39
3	357	8.6	41.51

Porosity from Image Processing

The gouge samples were imaged using backscattered SEM microscopy at magnifications up to 64K. Examples of telescopic imaging are shown in Figs. 2 and 3. Particles on deformed and undeformed gouge images were manually outlined and transformed onto line drawing overlays in Adobe Photoshop. The particle feret diameter and areas were measured on calibrated overlays using Sigma ScanPro© image processing software. The data was used to determine particle size distribution (PSD), and fractal dimension D. Porosity of the gouge from images were determined using thresholding techniques applied with a range of pixel intensities in order to include the highest and lowest possible porosities from each image.

The sources of error included image quality and magnification (imaging errors), and thresholding intensity assignment error. We estimate the total error to vary between 0.1 to 2% at the highest and lowest image magnifications respectively.

Fig. 2

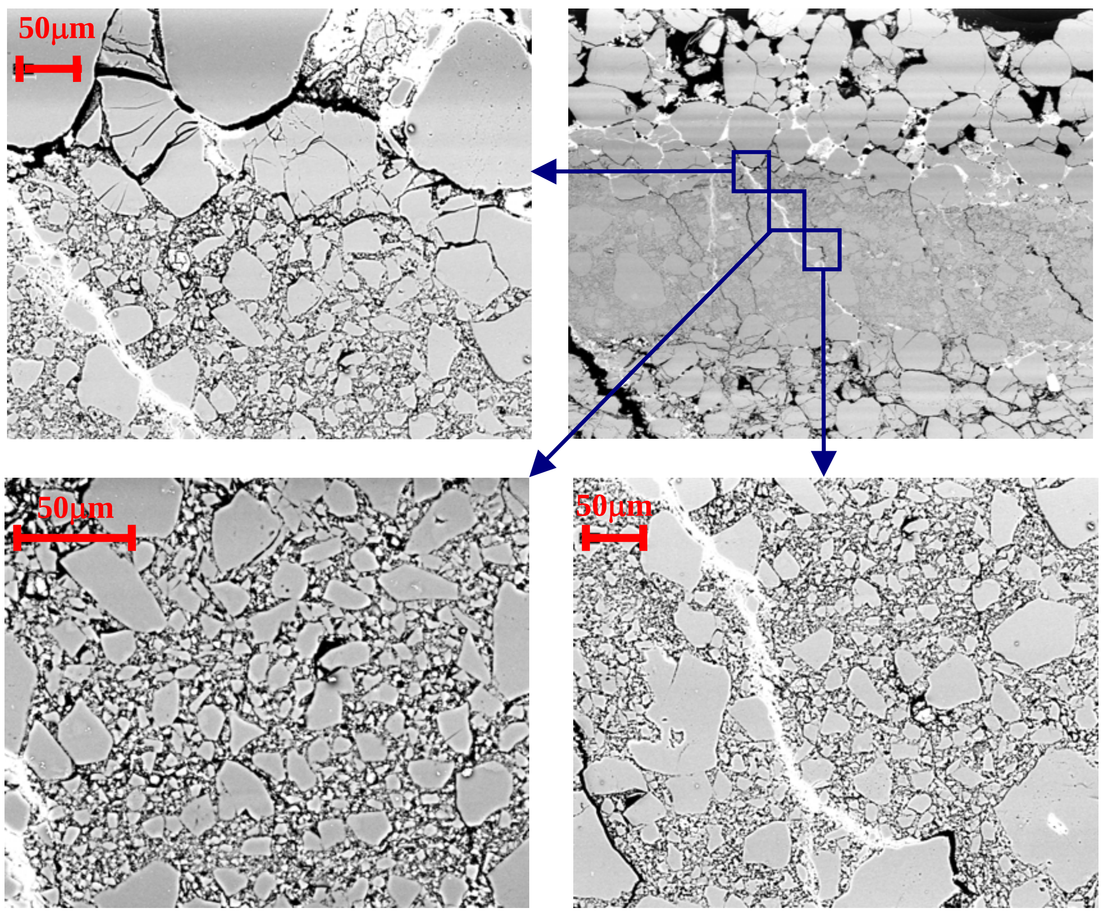

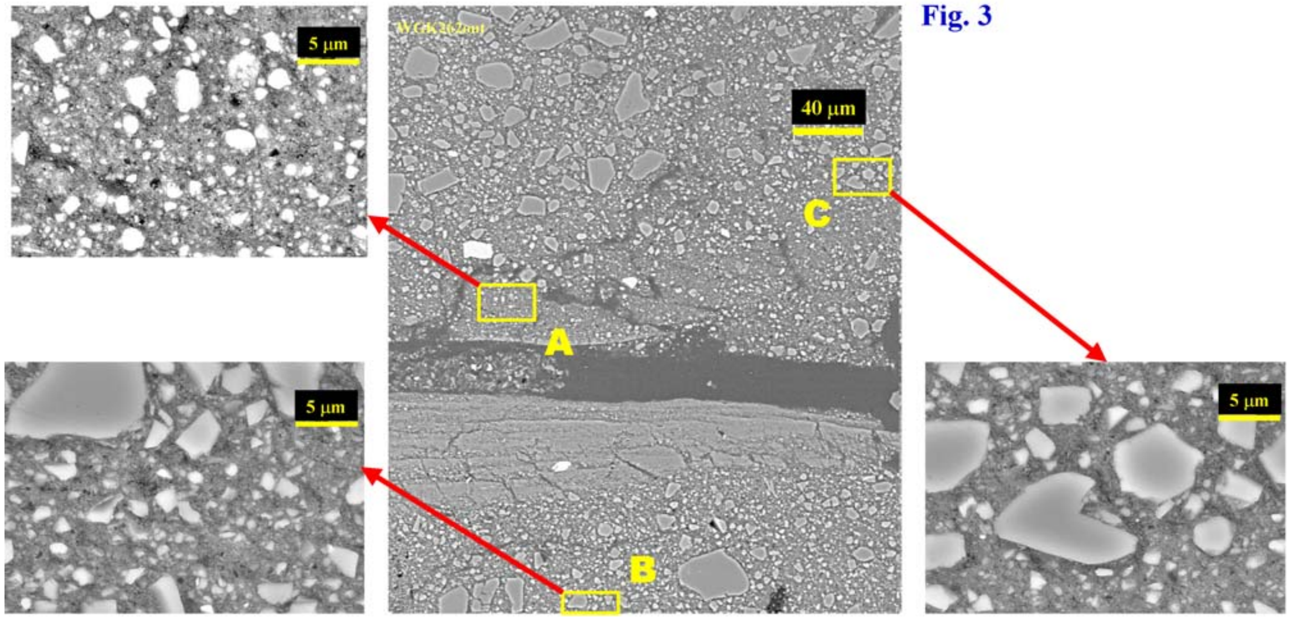

Fig. 3

Porosity Simulations

The simulation program written in VC++ is based on an algorithm that takes as input a set of size values acquired from gouge images. The gouge PSD was assumed to be fractal. The algorithm is capable of processing unlimited number of circular particles with unlimited size range in a descending order. However, different orders of the particle size data were tried as well. We used tangent circle solutions for packing the circles such that least number of the same size particles touch.

The output included numeric results, and the textural output via a visualizer. The simulated texture in Fig. 4 is for particle size data set from the image in Fig. 3 (region C). The 2D porosity of the simulated texture was calculated by summing up the void space areas. The program produces maximum packing density for the given data set under the described conditions.

The main source of error in the simulation originated with the manual particle outline tracing operation that created the particle size data. The accuracy of tracing in turn was dependent upon magnification and image quality. The tracing for all images were performed at 3 times frame magnification with 2 pixel lines in order to avoid significant errors.

Fig. 4

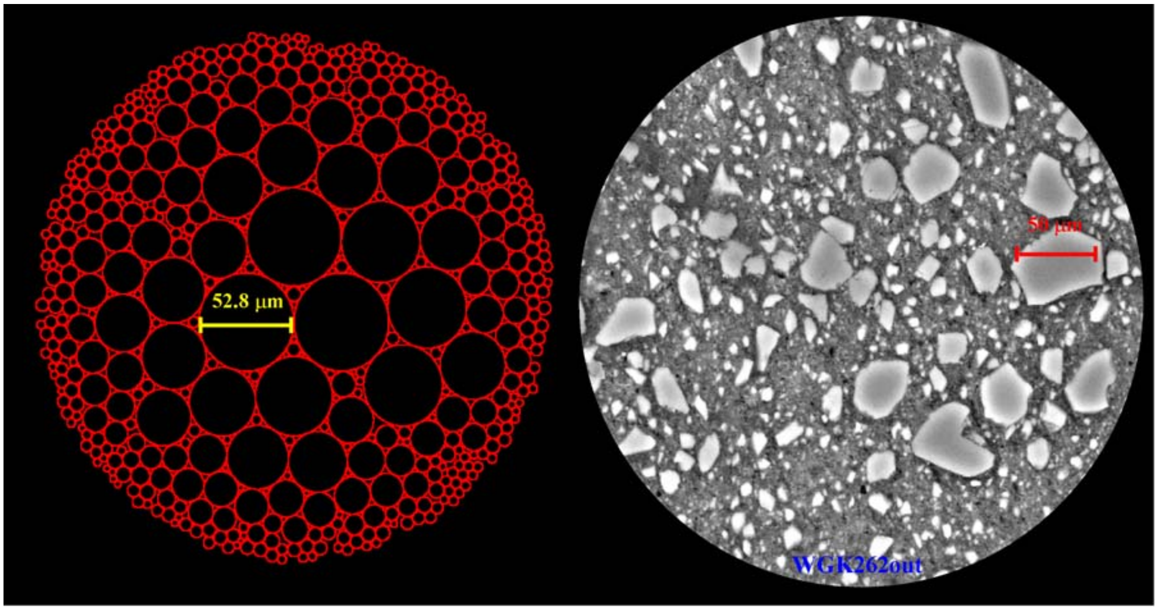

Typical simulated texture based on pooled particle size distribution data from 3 telescopic SEM images (1K, 2K, and 4K magnifications). Only the 1K image is shown. N = 528 particles.
Particles size range 0.4 µm to 52.8 µm. $\Phi_{\text{simulated}}$ = 0.47%; $\Phi_{\text{Image processing}}$ = 0.469%.

Results

The results in Tables 2 and 3 clearly show that there is a marked decrease in porosity and particle size with increasing shear displacement. Similar changes occur across R and Y slip surfaces in individual samples (constant displacement). The porosity value differences resulting from methodology is significant for the undeformed material, and is particularly high in the case of the simulated Westerly granite gouge (Fig. 1b), where the undeformed particles are angular to sub-angular (see I.P. vs. Simulation in Table 2). As shown in Figs. 5 and 6, these differences diminish rapidly with increased displacement. In both cases the porosity is reduced to a fraction of the undeformed porosity within the initial 10mm of shear displacement. The changes in fractal dimension appear to inversely follow those of the porosity and particle size (Fig. 7).

Table 2

WGK		δ (mm)	Φ I.P.	Φ Simulation	Particle data Number	Particle data Min (µm)	Particle data Max (µm)	Particle data D	Contact Points	γ
										0
									2769	22
	Outer region									
									545	39.5
									843	193.5
										193.5

Table 3

					Particle's data	Min (µm)	Max (µm)				γ
	13 (50)		21.84 Average between 11-20								0
				3.75	289	1.9	112.3	1.93	575		17
	3 (1k)		3.27		102		25		201		
				2.24	333	5	79.68	2.08	663		82.86
	1 (5k)		5.59		94		6.6		185		
				4.11	295	1.98	129.88	1.69	587		20.85
	3 (500)		4.91		221		87.7		439		
									1633		96.39
	1 (1k)		2.81	0.68	326	0.99	27.8	2.32	649		
					112		19.2		221		41.51
	4 (250)		3.19	4.03	163	2.5	112	2.14	323		

δ = Rotary shear displacement, mm
I.P. = % Porosity determined through image processing using telescopic SEM images.
D = slope of linear approximation to particle distribution

Φ = Porosity, percent; γ = Shear strain

Fig. 5

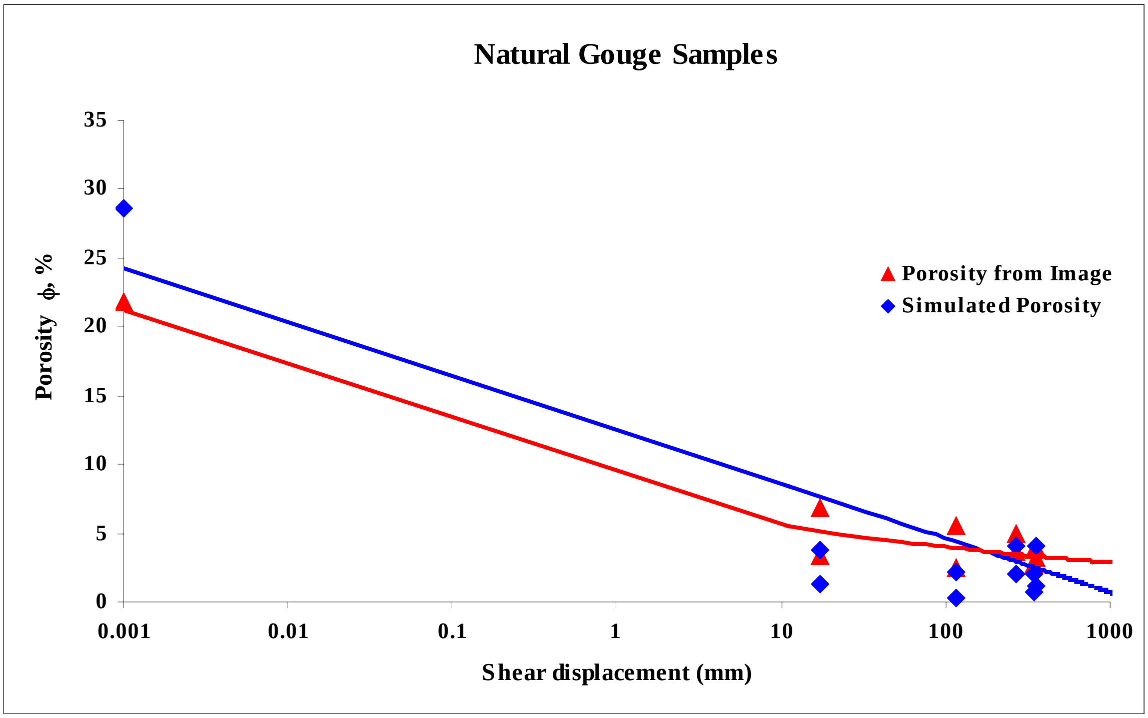
Natural Gouge Samples
Porosity ϕ, %
35
30
25
20
15
10
5
0
0.001
0.01
0.1
1
10
100
1000
Shear displacement (mm)
Porosity from Image
Simulated Porosity

Fig. 6

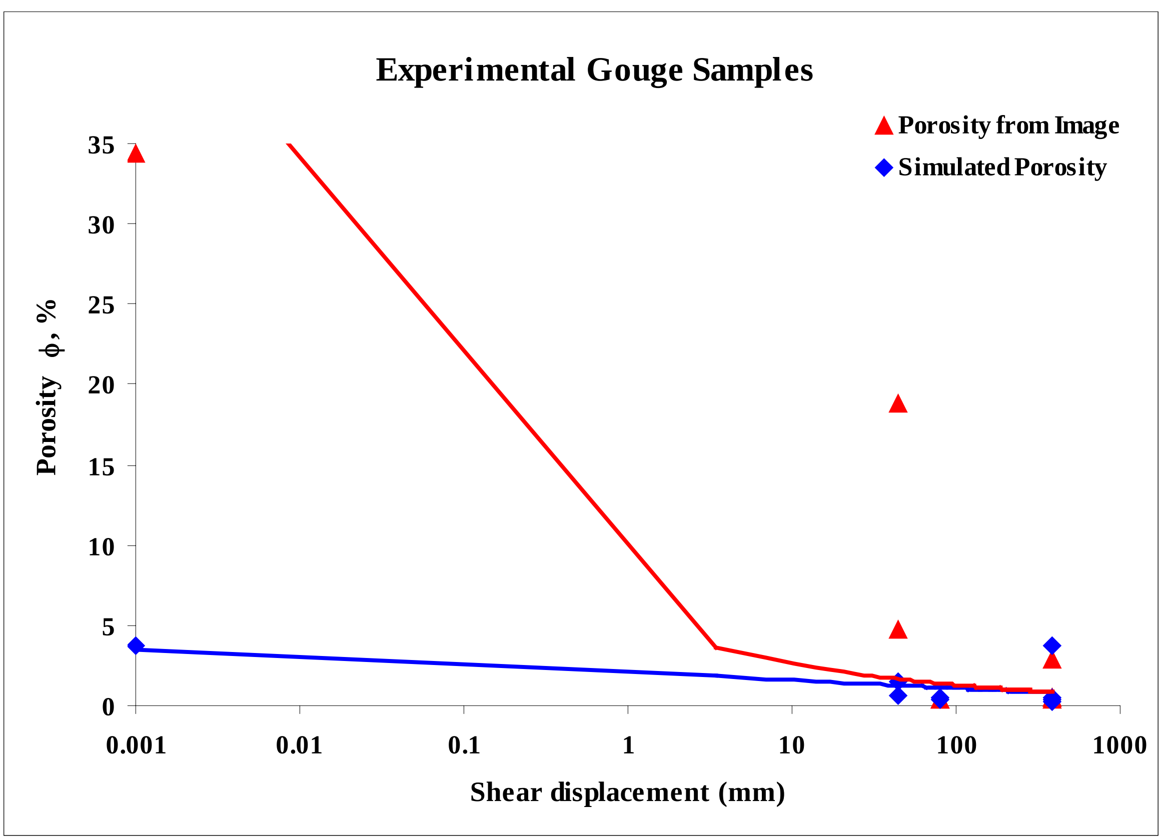
Experimental Gouge Samples
Porosity from Image
Simulated Porosity
Porosity ϕ, %
35
30
25
20
15
10
5
0
0.001
0.01
0.1
1
10
100
1000
Shear displacement (mm)

Fig. 7

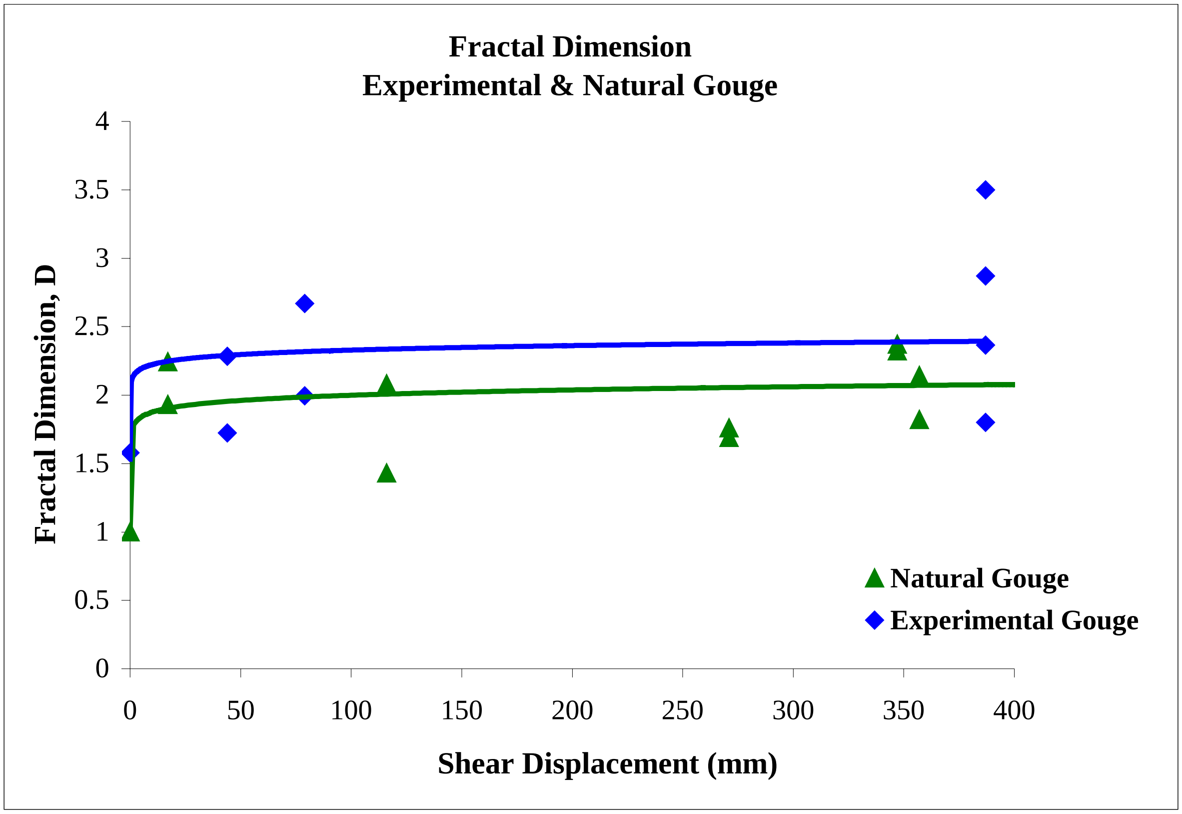

Interpretation

The results suggest that shear localization occurs early in the history of comminution and gouge particles tend to become rounded and equant in shape while reducing in size in and around the slip surfaces (Fig. 8). This appears to be true regardless of the gouge initial particle shapes and normal stress on the fault. The fractal dimension values from within zones of localization exceeds 2.58. In consequence, the gouge is highly densified within regions of localized shear.

Rutter and Hadizadeh (1991) showed that the low-temperature fracture to cataclastic flow transition pressure is strongly dependent on porosity (Fig. 9). Large, rapid reductions in local porosity under our sample conditions could result in a reverse transition to fracture at constant pressure. The mechanical effects include a positive change in friction during and prior to localization episodes, followed by weakening. The microstructural evidence of repeated gouge densification near Y slip surfaces and subsequent development of fracture-like features in the simulated Westerly granite gouge deformed to 79 mm of sliding is shown in Fig. 10.

Fig. 8

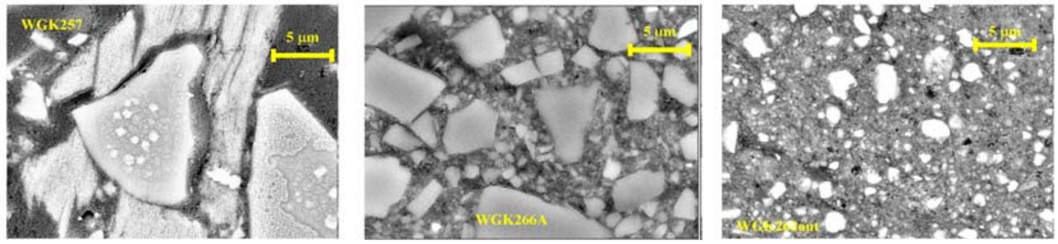
WGK257
5 µm
5 µm
WGK266A
5 µm

Fig. 9

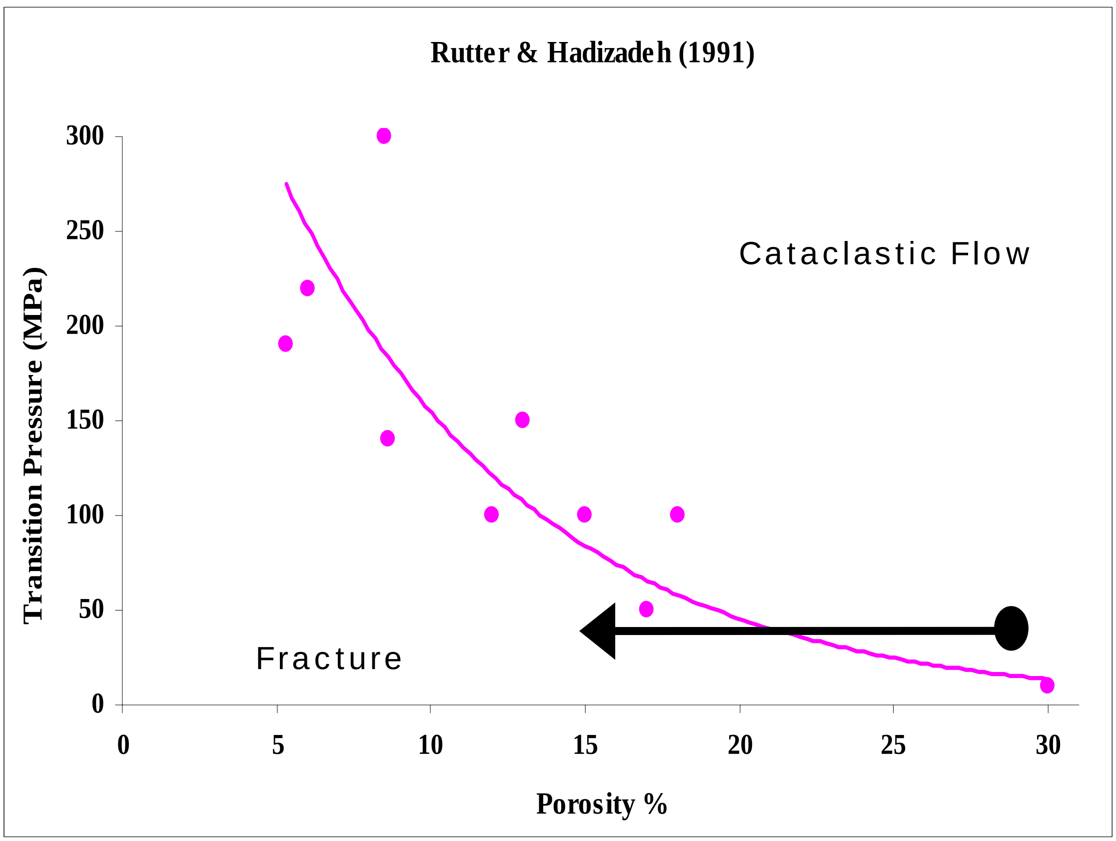
Rutter & Hadizadeh (1991)
Cataclastic Flow
Fracture
Transition Pressure (MPa)
Porosity %
0
50
100
150
200
250
300
0
5
10
15
20
25
30

Fig. 10

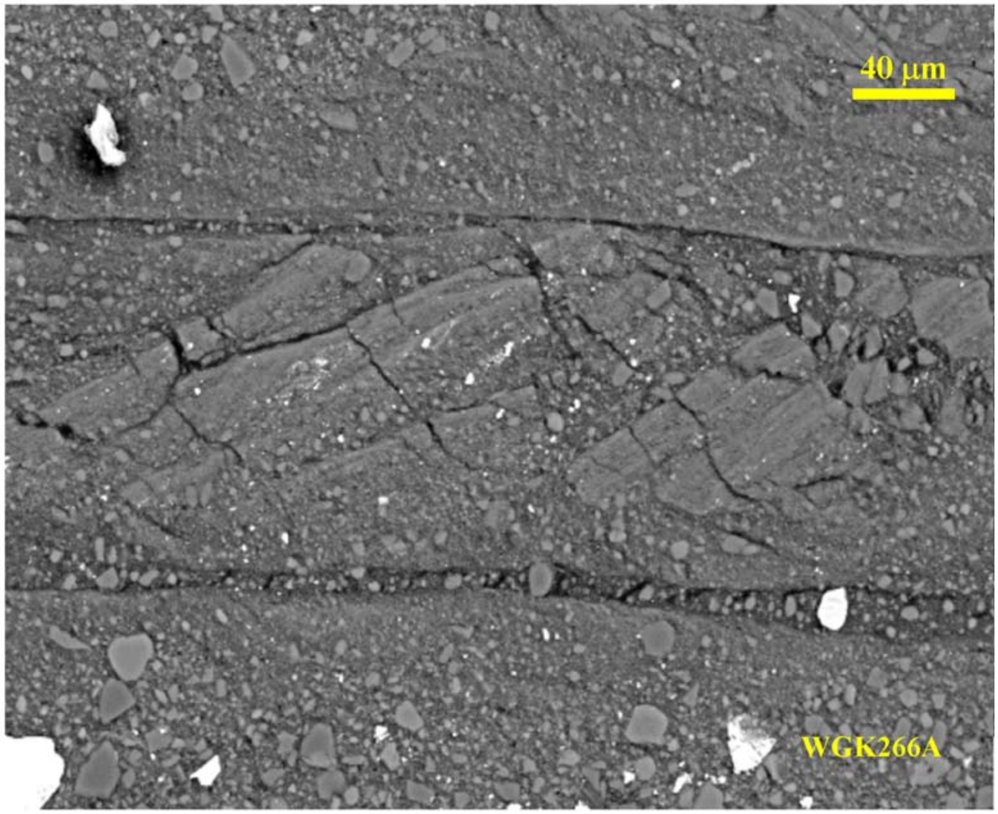

Conclusion

1.Fault gouge porosity decreases dramatically early in the history of comminution in areas of shear localization, resulting in packing density increases.
2. The particles tend to become more equant in shape as well as reduced in size across Y and R slip surfaces.
3. Based on brittle-ductile transition data for porous rock material the porosity reduction might result in local cataclastic flow to fracture transition along some slip surfaces in the gouge.

References

Rutter, E.H. & Hadizadeh, J., 1991, "On the influence of porosity on the low-temperature brittle-ductile transition in siliciclastic rocks", Journal of Structural Geology, 13, 609-614.
Flodin, E. & Aydin, A. 2004, "Evolution of a Strike-Slip Fault Network, Valley of Fire State Park, Southern Nevada. Geol. Soc. Amer. Bull., 116, 42-59.